American Mineralogist, Volume 88, pages 1145–1152, 2003

^{57}Fe Mössbauer-effect studies of Ca-rich, Fe-bearing clinopyroxenes: Part III. Diopside

EDDY DE GRAVE[1,*] AND SIGRID G. EECKHOUT[1,2]

[1]Department of Subatomic and Radiation Physics, Ghent University, B-9000 Gent, Belgium
[2]Department of Geology and Soil Science, Ghent University, B-9000 Gent, Belgium

ABSTRACT

Three natural Fe-bearing diopside samples, hereafter labeled Dp1, Dp2, and Dp3, have been examined by Mössbauer spectroscopy at temperatures from 4.2–800 K. The Fe contents are 0.01, 0.06, and 0.30 atoms per formula unit (apfu), respectively. All three species contain some Fe in the trivalent state. The spectra are adequately described by a superposition of three quadrupole doublets arising from Fe^{2+}(M1), Fe^{2+}(M2), and Fe^{3+}. The Fe^{3+} fraction seems to increase with increasing total Fe. The coordination of the ferric ions could not be inferred, but the observed line broadening of the Fe^{3+} doublet indicates that they possibly substitute at both M1 and M2. The ferrous ions have a strong preference for the M1 sites. For the ferroan diopside sample Dp3 a spectrum at 80 K in an applied field of 60 kOe was recorded to determine the signs and the asymmetry parameters of the electric-field gradient. The signs are all negative and the asymmetry is large (~0.9), implying that an additional distortion is superimposed on the trigonal compression of the polyhedra. The center shifts δ for the two Fe^{2+} sites are equal within experimental error limits. From their temperature variations, equal values for the lattice temperatures, Θ_M, and hence for their recoilless fractions, f_2, at any given temperature have been deduced. The recoilless fraction, f_3, for Fe^{3+} is higher. The f_2/f_3 ratio was found to be ~0.95 at 80 K, and decreases with increasing temperature. The temperature variations of the ferrous quadrupole splittings show the importance of spin-orbit coupling. They were calculated from the thermal populations of the 25 electronic levels within the ^5D term. The energies of these levels were determined by diagonalization of the complete crystal-field Hamiltonian. For the numerical expression of this Hamiltonian, use was made of the point-charge approach, which takes into account the real point symmetry of the M1 and M2 lattice sites by considering the positions and the effective charges of the various cations and anions in the diopside unit cell. The lattice contribution to the electric-field gradient and the spin-orbit coupling were included. We found that this theoretical treatment yielded excellent results for the M1 sites, correctly predicting the temperature dependencies of the quadrupole splittings for all three diopside species and the high magnitude of the asymmetry parameter. In contrast, the analyses for the M2 sites were less successful. We argue that the failure is due to a lack of correct crystallographic data concerning the coordination of Fe^{2+} at M2 in diopside.

INTRODUCTION

Diopside belongs to the group of Ca clinopyroxenes and the ideal formula is $CaMgSi_2O_6$. The structure is monoclinic, space group $C2/c$, with unit-cell parameters $a = 9.741$, $b = 8.919$, $c = 5.257$ Å, and $\beta = 105.97°$ (Sasaki et al. 1980). As in hedenbergite (see Part I and Part II), the Ca and Mg cations are located in eightfold (M2 sites) and sixfold (M1 sites) oxygen-coordination sites, respectively (Cameron and Papike 1980). The M2 sites are strongly distorted while the M1 sites have a more regular geometry. Commonly, natural diopside species are characterized by substitutions for Ca (e.g., by Na) and Mg (e.g., by Fe). The valence of the substituting Fe species is not exclusively restricted to Fe^{2+} and trivalent Fe may be present as well. If the abundance of Fe^{2+} or Fe^{3+} exceeds 0.10 apfu samples are termed as ferroan or ferrian diopsides, respectively (Morimoto 1988).

Fe-containing diopsides have been the subject of a number of different studies based on Mössbauer spectra (MS). Most of these studies, however, were concerned with hedenbergite-rich members of the solid-solution series $CaMgSi_2O_6$-$CaFeSi_2O_6$, generally written as $CaFe_xMg_{1-x}Si_2O_6$, whereas the diopside-rich side of the join has received little attention. Bancroft et al. (1971) reported MS recorded at 77 K, 210 K, and 295 K from a natural diopside with composition $Ca_{1.01}Fe_{0.05}Mg_{0.94}Si_2O_6$. They observed a single Fe^{2+} quadrupole doublet with parameters $\delta = 1.17$ mm/s (against α-Fe at 295 K) and $\Delta E_Q = 1.89$ mm/s at 295 K. Dollase and Gutstafson (1982) examined a synthetic sample with $x = 0.02$ ($Di_{98}Hd_{02}$) and similarly found at 295 K a ferrous quadrupole doublet with $\delta = 1.17$ mm/s and $\Delta E_Q = 1.85$ mm/s. In both cited studies the doublet was attributed to Fe^{2+} at the M1 sites. As far as we are aware, these are the only papers that consider Di-Hd samples that close to the diopside end-member.

* E-mail: eddy.degrave@rug.ac.be

As mentioned above, most attention in Mössbauer spectroscopy on Di-Hd samples has been focused toward hedenbergite-rich compositions along the tie line (see Part I for relevant references). Of particular interest for the present work are Di-Hd species exhibiting a shortage of Ca ions. Bancroft et al. (1971) reported for a magnesian hedenbergite with composition $Ca_{0.95}Mg_{0.20}Fe_{0.85}Si_2O_6$ two ferrous doublets ascribed to Fe^{2+}(M1) and Fe^{2+}(M2), respectively, the latter with an abundance of approximately 0.07 apfu. Both doublets have the same δ, but the quadrupole splittings and their temperature dependencies are quite different. For Fe^{2+}(M1), ΔE_Q varies from 2.71 mm/s at 77 K to 1.08 mm/s at 815 K, while in the same T range that for Fe^{2+}(M2) changes from 2.1 mm/s to 1.6 mm/s. This means that the $\Delta E_Q(T)$ curves "cross" somewhere in between the two extreme temperatures. This phenomenon has been observed for other clinopyroxenes as well, e.g., members of the enstatite–ferrosillite solid-solution series, where the "crossing" temperature, T_{cr}, for $Mg_{0.81}Fe_{0.19}SiO_3$ lies around 500 K (Eeckhout 2000). This crossing behavior is due to the higher degree of distortion of the axial symmetry of the M2 polyhedron as compared to the distortion of the M1 octahedron (Bancroft 1973).

Williams et al. (1971) examined two Ca-deficient Di-Hd samples at 77 K and 295 K. These authors found two doublets and assigned them to Fe^{2+}(M1) and Fe^{2+}(M2), in agreement with Bancroft et al. (1971). The ΔE_Q values specified in the two papers are reasonably similar. However, the changes in relative spectral areas, *RA*, of the two doublets in going from 77 K to 295 K as reported by Williams et al. (1971) are inconsistent in the sense that the doublet with the higher *RA* value at 77 K has a lower *RA* at 295 K. Bancroft (1973) mentioned a similar problem and argued that the shortcoming of the fit procedure is the result of the fact that both Fe sites are actually composed of several distinct components arising from non-uniform chemical environments of the probe nuclei. This means that the author somehow suggested that a model-independent quadrupole-splitting distribution (QSD) procedure, which was not yet developed in practice at that time, might be a more recommendable fitting approach. In Part I of these studies, we showed that such an approach did indeed lead to consistent Mössbauer results for hedenbergites over a very broad range of temperatures.

For the sake of completeness, it may be mentioned that ferrian diopsides have also been examined quite frequently by Mössbauer spectroscopy (Hafner and Huckenholz 1971; Nöller and Knoll 1983; Shinno and Maeda 1989; Skogby and Rossman 1989; De Grave and Van Alboom 1996; Redhammer 1998) as have Fe-bearing aluminum diopsides, formerly called "fassaites" (Kabalov et al. 1997; De Grave et al. 2002). The occurrence of QSD effects is particularly clear for the latter species.

The preceding, selective literature survey shows that the interpretation of the MS of $CaFe_xMg_{1-x}Si_2O_6$ clinopyroxenes, including diopsides, in the early seventies has remained merely qualitative and that in recent years no novel developments in that respect have been accomplished, despite the tremendous improvements in methodology and advanced computational methods. Moreover, systematic studies of diopside-rich species are lacking and consequently the temperature variations of the hyperfine parameters have remained unexplored. In this paper, the last part of a series of three focusing on the Mössbauer characteristics of Ca clinopyroxenes, the authors present their findings for three natural diopsides from which MS were recorded at many (~25) different temperatures in the range 4.2 K to 800 K.

Experimental methods

Three different diopside species, from private collections, have been considered in this study. Dp1 is a sample from Jaipur (India). The origin of Dp2 is unknown. Dp3 was collected from Zillertal, Tyrol (Austria). The powder X-ray diffraction patterns show that all three samples are single-phase diopsides. Qualitative elemental analyses were performed with the EDX technique making use of the ZAF correction. Elements other than Ca, Mg, Fe, and Si were not detected or were found as subordinate traces. Fe contents were of the order of 0.01, 0.04, and 0.30 apfu, respectively. For Dp1 a Ca deficiency could be concluded, but not so for Dp2 and Dp3. However, since no proper internal standards were used in the EDX analyses, no sound conclusion regarding the Ca balance in the latter two samples could be drawn. According to the classification of Morimoto (1988) Dp3 is a ferroan diopside species.

MS were recorded at various temperatures with a conventional, time-mode spectrometer operating in the constant-acceleration mode with a triangular reference signal. A total of 1024 channels were used for the accumulation of counts. The source was ^{57}Co(Rh). The velocity scale was periodically calibrated by taking spectra for a standard α-Fe foil at room temperature. All center-shift values quoted hereafter are with respect to this standard. The velocity increment per channel was ~0.016 mm/s. The absorbers consisted of the finely ground crystals, the powders being uniformly spread out over the support and sealed with an organic glue. The effective thickness was 5 mg Fe/cm^2 or less so that thickness effects are small. Low temperatures were obtained using commercial flow cryostats with a temperature control within ± 0.2 K. A vacuum furnace provided temperatures up to ~800 K. For the sample with the highest Fe concentration and the highest Fe^{3+}/Fe^{2+} ratio (Dp3) a MS was collected with the absorber held at 80 K and subjected to a longitudinal, external magnetic field of 60 kOe. The purpose of this experiment was to determine the signs of the electric-field gradient's (EFG) principal components, V_{zz}, acting at the various Fe sites. Knowledge of this feature is required to assess the axial term of the local symmetry of the respective sites (Bancroft 1973).

The zero-field MS, consisting of Fe^{2+} and Fe^{3+} contributions (see next section) were fit with a superposition of symmetrical (i.e., equal line width and intensity for the two partner lines in a given doublet), Lorentzian-shaped doublets. Generally, for each of the doublet components δ, ΔE_Q, *RA*, and Γ were all adjustable parameters. However, as will be detailed in the next section, restrictions on some of the parameter values had to be imposed in a few cases. The shape of the applied-field MS is very complicated and several restrictions had to be introduced in the fitting procedure. The line shapes of the distinct components and of their superposition were calculated by numerical diagonalization of the complete hyperfine-interaction Hamiltonian.

Results

Zero-field spectra

MS collected for Dp1 and Dp2 at selected temperatures are reproduced in Figure 1. In Part I of this series, dealing with hedenbergites, the authors based their interpretations of the temperature variations of the hyperfine interactions on the results obtained from quadrupole-splitting distribution (QSD) fits. Although discrete-doublet fits at first glance led to similar results for the various Mössbauer parameters, the temperature variations of these parameters, as derived from this latter method, eventually seemed to show some minor inconsistencies, which was not the case with the QSD approach. The crucial difference between the (paramagnetic) hedenbergite MS and the present Dp1 and Dp2 MS is that the latter spectra at high temperatures clearly exhibit shoulders on the outward slopes of the main absorption lines, which strongly suggests the presence of two discrete Fe^{2+} sites. In contrast, the Fe^{2+} component in the hedenbergite MS is merely broadened, but remains fairly symmetric, without fine structure, over the entire temperature scan.

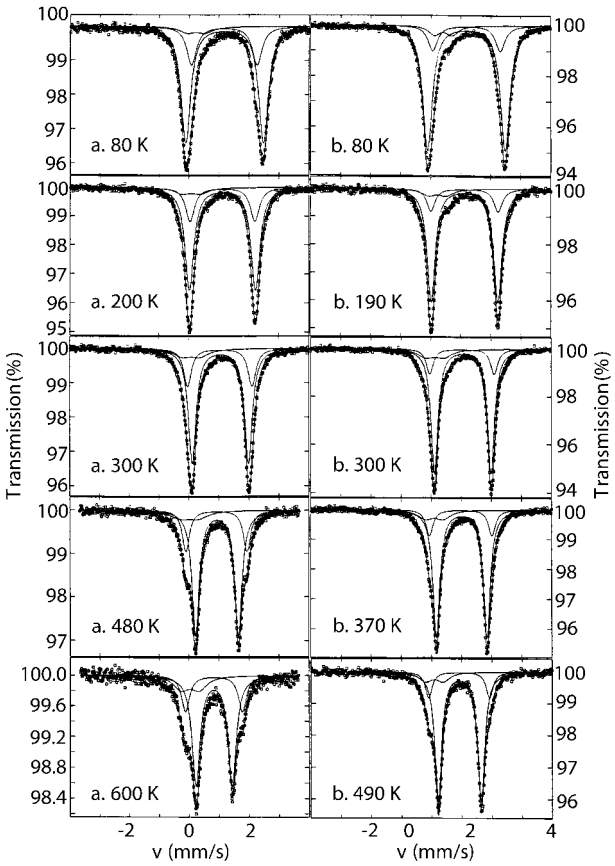

FIGURE 1. Mössbauer spectra at selected temperatures for diopsides Dp1 (**a**) and Dp2 (**b**). Solid lines reproduce the Fe^{2+}(M1), Fe^{2+}(M2), and Fe^{3+} quadrupole doublets and their superposition adjusted to the experimental data.

A superposition of two Fe^{2+} doublets and one weak Fe^{3+} doublet was found to provide adequate (see solid lines in Fig. 1) and consistent fits of the Dp1 and Dp2 MS. Numerical data for a limited selection of different temperatures and resulting from this discrete-doublet approach are presented in Table 1. They were obtained on the basis of constraints imposed in the fitting routine that will be presented and discussed at a later stage in this paper.

It should be mentioned at this point that the QSD approach used to analyze the hedenbergite MS in Part I was also used to fit the present diopside spectra. Not surprisingly, the evaluated distribution profiles of ΔE_Q for Dp1 and Dp2 clearly reflect the existence of two distinct and significant sub-components for Fe^{2+}, with extrema coinciding within experimental error limits with the ΔE_Q values of the corresponding ferrous doublets. For obvious reasons, the QSD fits resulted in somewhat lower goodness-of-fit (χ^2) values, i.e., slightly better fits. However, the improvements were not spectacular and the relevant Fe^{2+} Mössbauer-parameter values and their temperature dependencies did not differ significantly from the results of the three-doublet fits. Moreover, the inclusion of the Fe^{3+} component in the QSD fit was not always straightforward. Therefore, we believe that it is meaningful to report further details regarding the interpretations of the Mössbauer parameters based on their values obtained from the three-doublet fits.

For Dp3, having the highest Fe content among the presently studied diopside species, the Fe^{3+} contribution is clear (Fig. 2). The quadrupole splitting was found to be 0.54 ± 0.02 mm/s regardless of the temperature. The line width Γ is very broad (~0.5 mm/s at 300 K) and shows the tendency to increase with increasing temperature.

On the basis of literature suggestions, and supported by the presently observed temperature variations of the quadrupole splittings, the ferrous doublet with the higher ΔE_Q at low temperatures is attributed to the M1 sites, the other doublet to the more irregular M2 sites. The center shifts for the two Fe^{2+} sites are equal within experimental error limits, indicating that the coordination number is the same for these two sites. This find-

TABLE 1. Mössbauer parameters for the three doublets fitted to the experimental spectra of the three diopside species at selected temperatures (in K)

Sample		Fe^{2+}(M1)				Fe^{2+}(M2)*			Fe^{3+}		
	T	δ	ΔE_Q	Γ	*RA*	δ	ΔE_Q	*RA*	δ	Γ	*RA*
Dp1	4.2	1.30	2.53	0.40	0.71	1.29	2.15	0.24	0.40	1.04	0.05
	80	1.30	2.58	0.39	0.70	1.29	2.18	0.24	0.39	0.70	0.06
	200	1.23	2.20	0.36	0.69	1.23	2.16	0.23	0.35	0.84	0.08
	300	1.16	1.87	0.31	0.68	1.15	2.14	0.23	0.30	0.77	0.10
	500	1.02	1.38	0.32	0.66	1.02	2.00	0.22	0.25	0.52	0.12
	700	0.87	1.08	0.33	0.63	0.87	1.76	0.21	0.25	0.67	0.16
Dp2	30	1.30	2.56	0.54	0.80	1.30	2.26	0.17	0.60	0.46	0.03
	80	1.30	2.59	0.39	0.77	1.30	2.26	0.16	0.53	0.48	0.07
	190	1.23	2.22	0.33	0.76	1.23	2.24	0.16	0.36	0.65	0.08
	300	1.16	1.87	0.29	0.74	1.14	2.13	0.15	0.21	0.66	0.11
	490	1.04	1.42	0.28	0.75	1.02	2.02	0.15	0.19	0.54	0.10
Dp3	80	1.29	2.63	0.37	0.69	1.26	2.96	0.11	0.53	0.41	0.20
	200	1.23	2.29	0.38	0.70	1.19	2.78	0.11	0.49	0.40	0.19
	300	1.17	1.96	0.35	0.69	1.09	2.50	0.10	0.43	0.51	0.21
	480	1.05	1.49	0.37	0.69	0.97	1.84	0.10	0.27	0.66	0.21
	800	0.77	0.97	0.32	0.71	0.69	1.27	0.11	0.11	0.55	0.18

Notes: δ center shift vs. α-Fe and in mm/s (±0.01 mm/s for Fe^{2+} doublets, ±0.05 mm/s for Fe^{3+}), ΔE_Q quadrupole splitting in mm/s (±0.02 mm/s), Γ full width at half maximum (same for both Fe^{2+} doublets, ±0.02 mm/s), *RA* fractional spectral area (±0.02). The quadrupole spitting for the Fe^{3+} doublet was fixed at 0.55 mm/s for Dp1 and Dp2. *Assignment to M2 for Dp1 and Dp2 only; for Dp3 this doublet is also due to Fe^{2+}(M1)—see text.

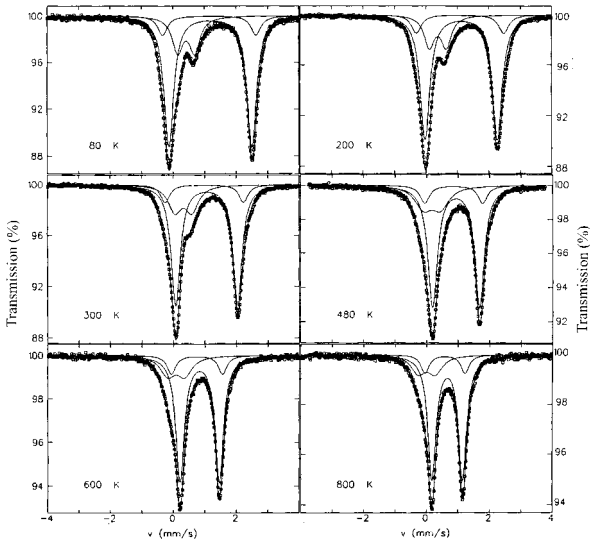

FIGURE 2. Mössbauer spectra at selected temperatures as indicated for diopside Dp3. Solid lines reproduce the Fe^{2+}(M1), Fe^{2+}(M2), and Fe^{3+} quadrupole doublets and their superposition adjusted to the experimental data. Note the increased contribution of Fe^{3+} (maximum absorptions at $v \approx 0.00$ mm/s and $v \approx 0.6$ mm/s).

ing consequently supports earlier studies on clinopyroxenes (Morimoto et al. 1960; Burnham 1966; Ohashi et al. 1975; Cameron and Papike 1980), which suggest that the coordination of M2 varies from six to eight depending on the size of the occupying cation, e.g., Fe and Ca, respectively.

As for Fe^{3+}, site assignment cannot be inferred from the Mössbauer data. Considering the broad line width, it is tempting to suggest that the ferric ions are at both M1 and M2 (the presence of Fe^{3+} at tetrahedral sites is very unlikely considering the high center-shift value, see Table 1). However, R^{3+} cations in pyroxenes are normally considered ordered with strong preference for the M1 positions (Cameron and Papike 1980). Therefore, the observed broadening of the ferric doublet might have one or more other reasons, for instance additional, nonuniform charge and site-geometry distortions of the Fe^{3+} M1 coordinations as a result of Fe^{3+} being normally not present in an ideal diopside structure. Thermal expansion of the lattice could then affect the extent of broadening.

For Dp1 and Dp2 the $\Delta E_Q(Fe^{3+})$ values obtained from the fits were much more scattered and a fixed and constant value of 0.55 mm/s, as found for Fe^{3+} in Dp3, was therefore imposed throughout the whole temperature range. We believe that due to the weak intensity of the ferric component, this constraint does not significantly affect any of the Fe^{2+} Mössbauer parameters.

Further, additional constraints had to be introduced to arrive at smooth and reasonable temperature variations of the various Mössbauer parameters for Dp1 and Dp2. At a certain temperature T_{cr} in the range 180–250 K the two ferrous doublets cross one another (see Fig. 1a where the crossing effect is most clear) and since their center-shift values are almost identical, the overlap of the two doublets is close to complete. No fitting routine can cope with such a situation. We found that forcing the two δ values to be equal, which is not an unreasonable assumption considering the lower- and higher-temperature results (Table 1) where the doublets are well resolved and no such constraints are required, and fixing the relative spectral areas at the average of the high-temperature values, provided excellent and consistent results. Figure 3 illustrates the crossing of the $\Delta E_Q(T)$ curves observed for Dp1 and Dp2.

Strangely, Dp3 does not show the crossing behavior and the two $\Delta E_Q(T)$ curves evolve more or less in parallel. For $P2_1/c$ Mg-Fe clinopyroxenes along the En–Fo join, which also exhibit crossing M1 and M2 $\Delta E_Q(T)$ curves, T_{cr} increases from ~500 K for $Mg_{0.81}Fe_{0.19}SiO_3$ to > 800 K for $FeSiO_3$ (Eeckhout 2000). This finding implies that the difference in distortion for M1 and M2, as quantified to first order by the difference in the energy gaps of the respective first-excited t_{2g} electronic levels, is smaller in end-member clinoferrosilite as compared to Mg-rich En–Fo clinopyroxene. Analogously, it is believed that for diopside the difference in distortion between M1 and M2 decreases with increasing Fe content. However, the presence of Fe^{3+}, which seems to be more pronounced for higher total iron, might additionally affect these behaviors.

Applied-field spectrum

The MS obtained for Dp3 at 80 K in an applied field, H_{ext} = 60 kOe, is reproduced in Figure 4. For the fit, the three Fe sites were taken into account. Their hyperfine parameters δ and ΔE_Q were fixed at the values derived from the zero-field MS at 80 K. Line widths, Γ, sign, SGN(eq), and asymmetry parameters, η, of the EFG, and fractional areas, RA, were allowed to vary in the iteration. In addition, three parameters for each Fe^{2+} doublet were adjustable, i.e., the anisotropic field-reduction parameters (negative) *HIX*, *HIY*, and *HIZ*, following the notation of Varret (1976). *X*, *Y*, and *Z* refer to the principal-axes frame of the EFG tensor. The meaning of these quantities is that if, e.g., the external field would be applied along the *z*-axis of the EFG, the field experienced by the nucleus would be H_{ext} + *HIZ*. The reductions are due to spin-polarization of the probe nuclei's *s*-electron clouds by the external field and are proportional to the corresponding components of the magnetic-susceptibility tensor (Johnson 1967). Since the Fe^{3+} is magnetically isotropic, only one field-reducing parameter has to be taken into account for this doublet.

The random orientation of the direction of the external magnetic field with respect to the EFG-axes frame was approxi-

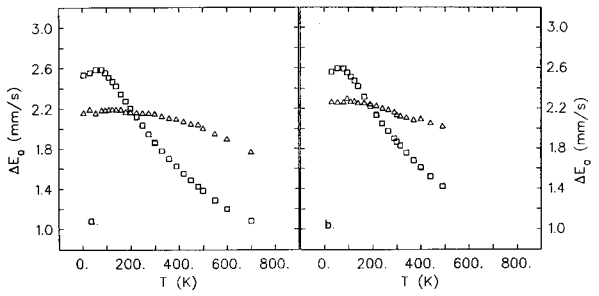

FIGURE 3. Temperature variations of the Fe^{2+} quadrupole splittings for Dp1 (**a**) and Dp2 (**b**) showing the "crossing" of the M1 and M2 curves around 200 K.

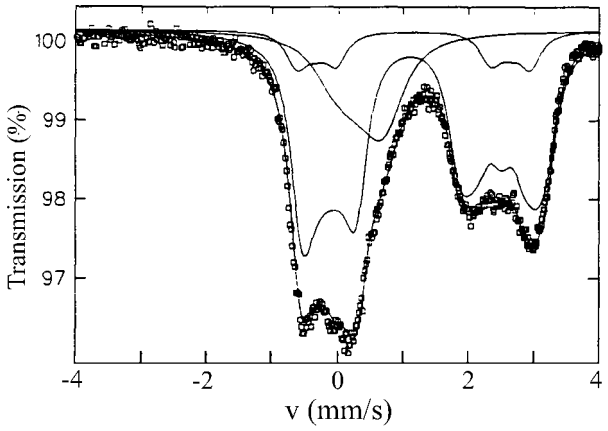

FIGURE 4. Applied-field spectrum of Dp3 at 80 K in a field of 60 kOe. The solid lines reproduce the Fe^{2+}(M1), Fe^{2+}(M2), and Fe^{3+} components and their superposition adjusted to the experimental data.

mated by a summation over discrete values of the polar and the azimuthal angles (θ, φ) (see Fig.2, Part II): 21 steps of 0.1 for cosθ, each value weighed by the $\sin^2\theta$ probability, and 18 steps for φ in the range 0° to 360°.

The results of the fitting procedure are listed in Table 2. For all three sites the sign of *eq* is negative and the site asymmetries are large. It is to be noted in this respect that η not only reflects the geometrical distortions of the respective O coordinations, but, also the asymmetry of the charge distributions in the neighboring cation shells. The values obtained for the fractional areas are in excellent agreement with the results from the zero-field spectrum, consequently supporting the applied fitting procedure.

The magnitude of the low-temperature quadrupole splittings (Table 1) and the negative sign of *eq* (presumed to be valid for all three diopsides, though of necessity only determined for Dp3) suggest that the first-order symmetry distortions of both the M1 and M2 sites are trigonal compressions (Ingalls 1964). Since the η parameter is quite high, additional, lower-symmetry distortions must be present, for instance a rhombic term as presumed to be the case for $P2_1/c$ (Fe, Mg) clinopyroxenes (Eeckhout et al. 2000).

The field reductions *HIX*, *HIY*, *HIZ* seem to be quite high. However, such high values are not unreasonable and not uncommon, and in some cases they can exceed the magnitude of the applied field (Varret 1976). For hedenbergite in an external field of 60 kOe at 80 K values are found of –37, –21, and –42 kOe, respectively (Eeckhout and De Grave 2003). In principle, one can calculate the reductions, provided that certain magnetic quantities are known, such as the saturation hyperfine field and the principal components of the tensors for the magnetic susceptibility and for the spectroscopic splitting factor. To the best of our knowledge these quantities have not been determined for Fe-bearing diopsides.

INTERPRETATION OF THE TEMPERATURE VARIATIONS OF THE HYPERFINE INTERACTIONS

Center shift δ

The center shifts for the two Fe^{2+} sites are equal within experimental error. The temperature dependencies, δ(*T*), for the three samples are reproduced in Figure 5 and have been interpreted in the usual manner, i.e., by assuming the Debye model for the lattice vibrations to approximate the temperature variation of the second-order Doppler shift (De Grave and Van Alboom 1991). In this approach, one parameter, i.e., the characteristic Mössbauer or lattice temperature, Θ_M, has to be adjusted in the iteration procedure. The solid lines in Figure 5 show the results of these calculations. No significant differences between the obtained Θ_M values (which are the same for M1 and M2) for the three diopside species could be detected, their magnitudes falling within the range 350 ± 10 K. Comparable values were previously reported for Mg-Fe ortho pyroxenes (Van Alboom et al. 1993) and Mg-Fe $P2_1/c$ clino pyroxenes (Eeckhout et al. 2000).

TABLE 2. Numerical data derived from the applied-field (60 kOe) Mössbauer spectrum of Dp3 at 80 K

Site	SGN(eq)	η	Γ	*HIX*	*HIY*	*HIZ*	RA
M1(Fe^{2+})	–	0.86	0.37	–34	–12	–30	0.70
M2(Fe^{2+})	–	0.97	0.35	–34	–35	–36	0.10
Fe^{3+}	–	0.96	0.67	–55	–55	–55	0.20

Note: sign SGN(eq) of the principal component eq of the electric-field gradient, asymmetry parameter η of the EFG (±0.05), line width Γ (in mm/s), field-reductions *HIX*, *HIY*, and *HIZ* (in kOe, ±5) and relative spectral area RA (±0.03) of the different Fe sites.

Figure 5 shows that the agreement between the experimental and calculated δ(*T*) curves is not complete, showing slight deviations in the high-temperature region, especially for sample Dp3. De Grave and Van Alboom (1991) argued that these deviations are attributable to a weak temperature dependence of the intrinsic isomer shift, δ_I, which is usually considered to remain constant, due to the radial expansions of the t_{2g} and e_g wave functions. Taking into account a linear correlation between δ_I and *T* as a first approximation, the high-temperature deviations are avoided. The as-such obtained Θ_M values turn out to be ~10% higher. A similar effect was found for species of hedenbergite. As a consequence of this temperature variation, the calculated Θ_M values, when including a linear correlation in the model, exceed the range 300–400 K as normally obtained for octahedrally coordinated Fe^{2+} (De Grave and Van Alboom 1991) under the assumption that δ_I has a constant value. The slope of the linear correlation between δ_I and *T* was found to be $\sim -4.5 \times 10^{-5}$ mm/(s.K), which is in line with earlier results for hedenbergite (De Grave and Van Alboom 1991)

The center-shift data for the Fe^{3+} doublets in Dp1 and Dp2 are relatively ill defined and the obtained temperature variations are not smooth. This explains why the model for interpreting the δ(*T*) curves yielded unrealistic or out-of-line values for Θ_M. For Dp3, where the ferric doublets in the MS are better resolved, the numerical treatment yielded Θ_M = 545 K, which is consistent with the values that have been found for octahedral Fe^{3+} in various other mineral species and also in synthetic samples (De Grave and Van Alboom 1991).

From the known values of Θ_M the recoilless fractions *f* at any given temperature can be calculated (De Grave and Van Alboom 1991). Assuming that the ferric ions in all three Dp species exhibit the same Θ_M value, the *f* factors at 80 K are f_2 = 0.88 and f_3 = 0.93 for Fe^{2+} (at M1 and M2) and Fe^{3+}, respectively. The f_2/f_3 ratio is ~0.95 and decreases with increasing

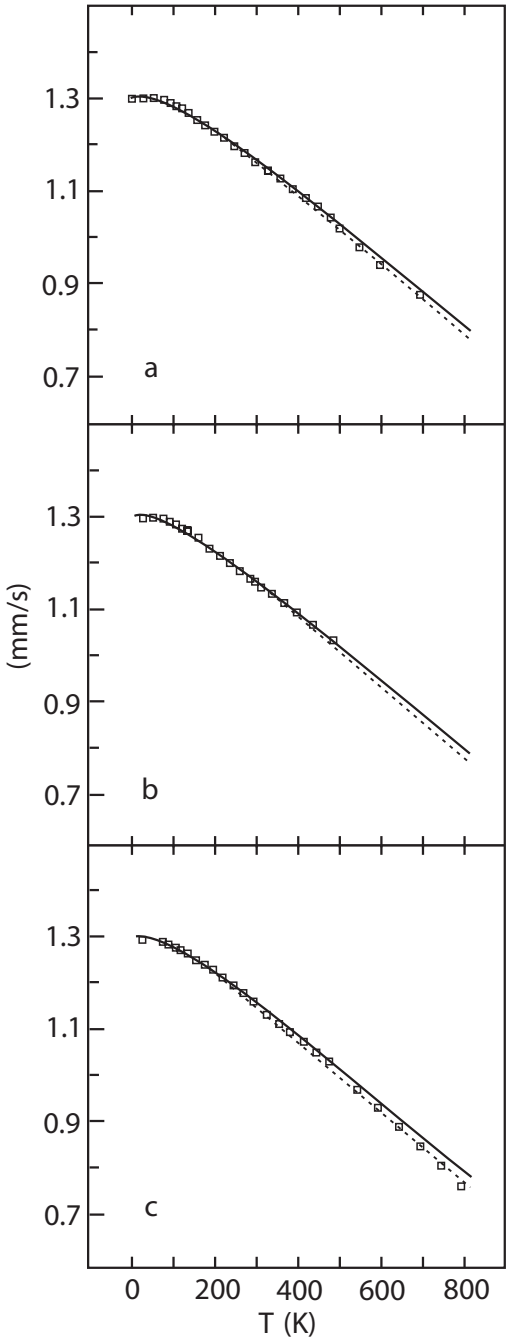

FIGURE 5. Temperature variations of the center shifts δ of the ferrous ions in Dp1 (**a**), Dp2 (**b**), and Dp3 (**c**). Note that Fe^{2+}(M1) and Fe^{2+}(M2) have equal δ values within experimental error limits. Solid lines are calculated curves assuming the intrinsic isomer shifts to be constant with temperature. The dotted lines represent the results in the case that a linear correlation between the intrinsic isomer shift and the temperature is included in the model.

temperature. This finding can be attributed to the higher valence state of Fe^{3+} resulting in stronger bonds to the O ligands. Theory is obvious in that the difference between f_3 and f_2 increases with increasing T. This explains why the RA values of the ferric doublets increase with increasing T (Table 1). Based on these values for the f factors and on the RA data at 80 K, the Fe^{3+}/Fe_{tot} ratios were found to be 0.05, 0.07, and 0.19 for Dp1, Dp2, and Dp3, respectively. From this observation the suggestion might emanate that higher amounts of Fe tend to favor the formation of Fe^{3+} at the expense of Fe^{2+}. However, since only three samples have been examined the correlation could be fortuitous. In general, Fe^{2+}/Fe^{3+} ratios in minerals are sensitive to a multitude of external parameters such as O atom fugacity, pressure, and temperature at the time of mineral formation, presence of other substitutional ionic species, thermal histories of the involved samples, and so on.

Quadrupole splitting ΔE_Q: M1 sites

Unlike for the $P2_1/c$ (Fe, Mg) clinopyroxenes (Eeckhout et al. 2000), the temperature variations $\Delta E_Q(T)$ of the Fe^{2+} sites for the involved diopsides are observed to exhibit a maximum at $T \approx 80$ K, which is especially clear and significant for the M1 coordinations. The occurrence of a maximum in the $\Delta E_Q(T)$ curve is the result of the spin-orbit coupling and the importance of this effect has also been found for, among others, the M1 sites in orthopyroxenes (Van Alboom et al. 1993) and hedenbergites (Eeckhout and De Grave 2003). This kind of behavior implies that the simple analytical treatment of $\Delta E_Q(T)$, with a rhombic distortion added to the trigonal compression and subsequently calculating $\Delta E_Q(T)$ from the Boltzmann populations of the five Fe^{2+} electronic energy levels within the ^5D term, as was successfully done earlier for the $P2_1/c$ (Fe, Mg) clinopyroxenes (Eeckhout et al. 2000), can strictly spoken not be applied in the case of the presently studied diopsides.

To interpret the temperature variations of the quadrupole splittings (and also of the EFG asymmetry parameters) ab initio calculations were carried out to determine the crystal-field Hamiltonian (CFH), including the spin-orbit term (λ**L.S,** with **L** and **S** the orbital and spin vector operators) for the ferrous ions at the M1 sites in the diopside structure. These calculations were based on a point-charge approach (Van Alboom et al. 1993) using the crystallographic data of Sasaki et al. (1980) concerning the average charge of the ligands (1.313 e) and the average ligand-M1 cation distance (2.07 Å) in diopside. Furthermore, the electronic transition observed at 9730 cm^{-1} in the optical absorption spectrum of a diopside containing $x = 0.02$ Fe and attributed to the transition from the e_g electronic levels to the ground state (White and Keester 1966), was taken into account. The energy of this transition, commonly denoted as 10Dq, is proportional to the quantity $\langle r^4 \rangle$, the expectation value of the fourth power of the radial part of the 3d wave function, which appears in the quantum-mechanical expression of the CFH. It was thus found that $\langle r^4 \rangle = 18.5$ a.u. Once the CFH has been constructed, diagonalization of it yields the energies of the various electronic levels within the ^5D term and from these the valence contribution to the quadrupole splitting at any given temperature can be calculated from the Boltzmann populations of the respective levels. The value used for the nuclear quadrupole moment, Q, was +0.15 barn and the Sternheimer shielding factor, $R = 0.12$ (Lauer et al. 1979). The zero-Kelvin, free-ion Fe^{2+} valence term, $\Delta E_{o,free} = 2e^2Q(1-R)\langle r^{-3} \rangle/7$ was fixed at 3.76 mm/s based on the value $\langle r^{-3} \rangle = 4.93$ a.u. reported by Freeman and Watson (1965). For Fe^{2+} bound to anions in a crystal, this free-ion value is reduced

by a factor α^2 due to covalence effects.

In addition to the valence contribution to the EFG, there is also a contribution from the distribution of the more distant charges within the lattice. This contribution was estimated by lattice summations of the theoretical expression for the EFG created by a point charge placed at a given position with respect to the probe nucleus (Nozik and Kaplan 1967). The calculations were extended to distances beyond which further lattice summations did not change the result to any significant extent. The Sternheimer anti-shielding factor, $\gamma\infty$, was chosen to be –10.97 (Lauer et al. 1979).

In the final iteration procedure within the point-charge model, two parameters were adjusted: the covalence factor a^2 and the radial quantity $\langle r^2 \rangle$. The fit was repeated for several fixed values for the spin-orbit-coupling constant, l, varied with steps of 5 cm^{-1}. The results for l = 45 cm^{-1}, are illustrated in Figure 6, showing an excellent agreement between the observed temperature variations of the M1(Fe^{2+}) quadrupole splittings and the calculated curves for all three diopside species involved. The negative sign of eq (Table 2), was confirmed by the calculations. Moreover, the high value of the asymmetry parameter h as derived from the applied-field MS of Dp3 at 80 K is well reproduced. One shortcoming is the low magnitude of the spin-orbit-coupling constant l, which is commonly around –60 to –70 cm^{-1} (e.g., Eeckhout and De Grave 2002); Van Alboom et al. 1993). The adjusted parameter values are listed in Table 3, together with some relevant energy values of the electronic levels, which are calculated from the diagonalization of the CFH. These are the energy gaps between the middle level within the spin-orbit-splitted singlet ground state of the t_{2g} level and the middle levels of the two quintets of the excited e_g state, E_7 and E_{12}, respectively. It is clear that the Fe^{3+} content does not affect the electronic level scheme of the M1(Fe^{2+}) cations. For completeness, the energy gaps E_{17} and E_{22} referring to the excited e_g levels are included as well.

It is interesting to compare at this point the diopside M1 level schemes with those obtained for hedenbergites (see Part I of these studies). This comparison shows that there is no significant difference in the energy splittings of the t_{2g} levels, inferring that the Fe / (Fe + Mg) ratio has no measurable effect on the symmetry distortions of the M1 coordinations. In addition, the Θ_M values are not substantially affected by Fe / (Fe + Mg), leading to the conclusion that the average Fe-O(M1) bond strength does not change with composition along the diopside–hedenbergite line.

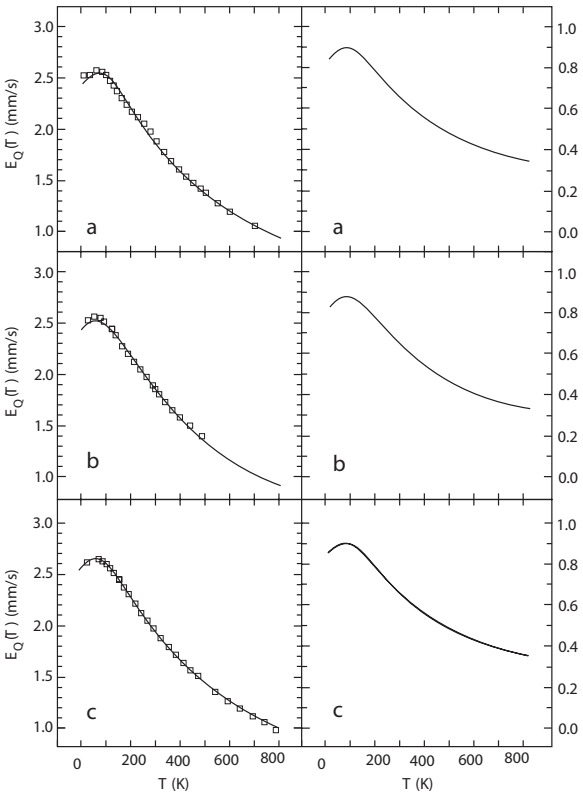

FIGURE 6. Experimental and calculated (solid line) temperature variations of the M1 ferrous quadrupole interactions $\Delta E_Q(T)$ (**a**) and calculated asymmetry parameter $\eta(T)$ of the EFG (**b**) for the three diopside species (from top to bottom: Dp1, Dp2, Dp3). Note that the observed value of η at 80 K for Dp3 is ~0.9.

Quadrupole splitting ΔE_Q: M2 sites

The point-charge model was also applied in an attempt to explain the temperature variations of ΔE_Q of the Fe^{2+}(M2) ions. These attempts were unsuccessful, since either the adjusted parameter values had unreasonable values, or the calculated $\Delta E_Q(T)$ curves did not reproduce the observed values in an adequate manner. We note that, although Fe preferentially substitutes at M1, a significant portion occurs at the more distorted M2 sites (Table 1), and hence, the hyperfine parameters for Fe^{2+}(M2) are well defined. We believe that the reason for the failure lies in erroneous crystallographic data concerning the Fe^{2+}(M2) coordinations. The data of Sasaki et al. (1980) indeed refer to M2 sites that are occupied by Ca^{2+}. If Ca is replaced by smaller Fe^{2+} ions, then a significant change in the geometry of the ligands is likely to occur. This reasoning is supported by several earlier studies on clinopyroxenes that report on a change of the coordination number of the M2 sites from eight to six when Ca^{2+} is substituted for smaller cations, such as Fe^{2+} and Mg^{2+} (Morimoto et al. 1960; Burnham 1966; Ohashi et al. 1975; Cameron and Papike 1980). The relative positions of the M1 ligands remain nearly unchanged in this transformation. In particular, when in hedenbergite or in diopside Ca^{2+} is entirely replaced by Fe^{2+} or Mg^{2+}, respectively, the crystal structures transform from the monoclinic forms to the corresponding orthorhombic forms, namely orthoferrosillite and orthoenstatite, respectively. However, although the crystal structures of, e.g., orthoferrosillite (*Pbca*) and clinoferrosillite (*C*2/*c*) are different, the relative positions of the cations in the unit cell show a remarkable resemblance (Burnham 1966). Taking this feature into account, and considering the earlier finding that the Fe^{2+}(M2) $\Delta E_Q(T)$ curves for orthopyroxenes are adequately described within the point-charge model using the crystallographic data for orthoferrosillite (Van Alboom et al. 1993), it was not unreasonable to assume that the Fe^{2+}(M2) coordinations in Fe-bearing diopsides exhibit local structural characteristics that are very similar to those in orthopyroxenes. However, using the crystallographic and effective-charge data

TABLE 3. Results concerning the ^5D level scheme and the electric field gradient EFG for Fe^{2+} (M1) in Dp1, Dp2, and Dp3 as obtained from the temperature variation of the quadrupole splitting based on point-charge calculations including the lattice contribution and spin-orbit coupling ($\lambda = -45 cm^{-1}$)

Sample	$<r^2>$	$<r^4>$	ΔE_0	α^2	η	Δ_{oct}	E_7	E_{12}	E_{17}	E_{22}
Dp1	2.35	18.5	2.93	0.78	0.89	9520	320	780	9,200	10,300
Dp2	2.32	18.5	2.94	0.78	0.89	9520	320	780	9,200	10,300
Dp3	2.36	18.4	3.02	0.80	0.90	9470	320	780	9,100	10,300

Notes: Proportionality factors $<r^2>$ and $<r^4>$ (a.u.), quadrupole-coupling constant ΔE_0 (mm/s), covalence factor α^2, asymmetry parameter η at 80 K, cubic level splitting of the ^5D ground term in an octahedral crystal field Δ_{oct} (cm^{-1}), energies with respect to ground state of the middle levels of the spin-orbit quintuplets of the first E_7, second E_{12}, third E_{17}, and fourth E_{22} excited orbital states (cm^{-1}).

reported for orthoferrosillite (Sasaki et al. 1982), this procedure produced results of which some were still believed to be inconsistent, although the reproductions of the experimental $\Delta E_Q(T)$ curves were fairly reasonable. Nevertheless, the authors find it wise to specify no further details in this paper.

In summary, as far as the fully detailed interpretation of the $\Delta E_Q(T)$ curves for the Fe^{2+}(M2) sites in these Fe-bearing diopsides is concerned, more precise crystallographic data for these sites must become available in order that the point-charge model can be applied successfully. It is worth mentioning at this point that for several representative clinopyroxenes a significant residual electron density, centered close to the M2 sites, has been inferred from X-ray structure refinement. According to Rossi et al. (1987) this phenomenon is due to an off-center displacement of the relatively small-sized Fe^{2+} cations (0.77 Å) within the M2 polyhedron, whose size is mainly dictated by the large Ca and Na species (~1.0 Å). This residual electron density may have an effect on $\Delta E_Q(T)$ not accounted for by the applied point-charge modeling. However, including this off-center density in the model seems at first glance to be a complicated task and no attempts in that respect have been undertaken in the present study.

ACKNOWLEDGMENTS

The authors thank the Fund for Scientific Research–Flanders for its continuous financial support, which has made this research project feasible. A. Van Alboom is acknowledged for his assistance in interpreting some of the reported data.

REFERENCES CITED

Bancroft, G.M. (1973) Mössbauer Spectroscopy : An Introduction for Inorganic Chemists and Geochemists. 252 p., McGraw-Hill, London.

Bancroft, G.M., Williams, P.G.L., and Burns, R.G. (1971) Mössbauer spectra of minerals along the diopside – hedenbergite tie line. American Mineralogist, 56, 1617–1625.

Burnham, C.W. (1966) Ferrosillite. Carnegie Institution Washington Year Book, 65, 285–290.

Cameron, M. and Papike, J.J. (1980) Crystal chemistry of silicate pyroxenes. In C.T. Prewitt, Ed., Pyroxenes, p. 1–92. Reviews in Mineralogy, Mineralogical Society of America, Washington, D.C.

De Grave, E. and Van Alboom, A. (1991) Evaluation of ferrous and ferric Mössbauer fractions. Physics and Chemistry of Minerals, 18, 337–342.

——— (1996) Mössbauer effect study of synthetic ferrian diopsides. In I. Ortalli, Ed., Proceedings of the International Conference on the Applications of the Mössbauer, p. 729–732, SIF, Bologna.

De Grave, J., De Paepe, P., De Grave, E., Vochten, R., and Eeckhout, S.G. (2002) Mineralogical and Mössbauer spectroscopic studies of a diopside occurring in the marbles of Andranondambo, southern Madagascar. American Mineralogist, 87, 132–141.

Dollase, W.A. and Gustafson, W.I. (1982) ^{57}Fe Mössbauer spectral analysis of the sodic clinopyroxenes. American Mineralogist, 67, 311–327.

Eeckhout, S.G. (2000) High-pressure synthesis, mineralogical characterisation and Mössbauer study of the solid-solution series enstatite-ferrosilite [$MgSiO_3$-$FeSiO_3$]. 140 p., Ph.D. dissertation, Ghent University.

Eeckhout, S.G. and De Grave, E. (2003) ^{257}Fe Mössbauer-effect studies of Ca-rich, Fe-bearing clinopyroxenes: Part I. Paramagnetic spectra of magnesian hedenbergite. American Mineralogist, 88, 1128–1137

Eeckhout, S.G., De Grave, E., McCammon, C.A., and Vochten, R. (2000) Temperature dependence of the hyperfine parameters in synthetic $P2_1/c$ Mg-Fe pyroxenes along the $MgSiO_3$ – $FeSiO_3$ join. American Mineralogist, 85, 943–952.

Freeman, A.J. and Watson, R.E. (1965) Hyperfine interactions in magnetic materials. In G.T. Rado, and H. Suhl, Eds., Magnetism IIA, p. 167–305. Academic Press, New York.

Hafner, S.S. and Huckenholz, H.G. (1971) Mössbauer spectrum of synthetic ferridiopside. Nature Physical Science, 233, 9–11.

Ingalls, R. (1964) Electric field gradient tensor in ferrous compounds. Physical Review, 133A, 784–795.

Johnson, C.E. (1967) Hyperfine Interactions in ferrous fluosilicates. Proceedings of the Physical Society, 92, 748–757.

Kabalov, Y.K., Oeckler, O., Sokolova, E.V., Mironov, A.B., and Chesnokov, B.V. (1997) Subsilicic ferrian aluminian diopside from the Chelyabinsk coal basin (southern Urals)—an unusual clinopyroxene. European Journal of Mineralogy, 9, 617–621.

Lauer, S., Marathe, V.R., and Trautwein, A. (1979) Sternheimer shielding using various approximations. Physival Review, A19, 1852–1861.

Morimoto, N. (1988) Nomenclature of pyroxenes. American Mineralogist, 73, 1123–1133.

Morimoto, N., Appleman, D.E., and Evans, H.T. (1960) The crystal structures of clino-enstatite and pigeonite. Zeitschrift fur Kristallographie, 114, 120–147.

Nöller, R. and Knoll, H. (1983) Magnetic properties of calcium-silicates (diopside and gehlenite) doped with Fe(III). Solid State Communications, 47, 237–239.

Nozik, A.J. and Kaplan, M. (1967) Significance of the lattice contribution to Mössbauer quadrupole splitting : Re-evaluation of the Fe^{57m} nuclear quadrupole moment. Physical Review, 159, 273–276.

Ohashi, Y., Burnham, C.W., and Finger, L.W. (1975) The effect of Ca – Fe substitution on the clinopyroxene crystal structure. American Mineralogist, 60, 423–434.

Redhammer, G.J. (1998) Mössbauer spectroscopy and Rietveld refinement on synthetic ferri-Tschermak's molecule $CaFe^{3+}(Fe^{3+}Si)O_6$ substituted diopside. European Journal of Mineralogy, 10, 439–452.

Rossi, G., Oberti, R., Dal Negro, A., Molin, G.M., and Mellini, M. (1987) Residual electron density at the M2 site in C2/c clinopyroxenes: relationships with bulk chemistry and sub-solidus evolution. Physics and Chemistry of Minerals, 14, 514–520.

Sasaki, S., Fujino, K., Takéuchi, Y., and Sadanaga, R. (1980) On the estimation of atomic charges by X-ray method for some oxides and silicates. Acta Crystallographica, A36, 904–915.

Sasaki, S., Takéuchi, Y., Fujino, K., and Akimoto, S. (1982) Electron-density distribution of three orthopyroxenes, $Mg_2Si_2O_6$, $Co_2Si_2O_6$, and $Fe_2Si_2O_6$. Zeitschrift für Kristallographie, 158, 279–297.

Shinno, I. and Maeda, Y. (1989) Mössbauer spectra of diopside containing 4- and 6-coordinated ferric irons at 78 K and 4.2 K. Mineralogical Journal, 14, 191–197.

Skogby, H. and Rossman, G.R. (1989) OH^- in pyroxene : An experimental study of incorporation mechanisms and stability. American Mineralogist 74, 1059–1069.

Van Alboom, A., De Grave, E., and Vandenberghe, R.E. (1993) Study of the temperature dependence of the hyperfine parameters in two orthopyroxenes by ^{57}Fe Mössbauer spectroscopy. Physics and Chemistry of Minerals, 20, 263–275.

Varret, F. (1976) Mössbauer spectra of paramagnetic powders under applied field: Fe^{2+} in fluosilicates. Journal of Physics and Chemistry of Solids, 37, 265–271.

White, W.B. and Keester, K.L. (1966) Optical absorption spectra of iron in the rock-forming silicates. American Mineralogist, 51, 774–791.

Williams, P.G.L., Bancroft, G.M., Bown, H.G., and Turnock, A.C. (1971) Anomalous Mössbauer spectra of *C2/c* clinopyroxenes. Nature Physical Science, 230, 149–151.

MANUSCRIPT RECEIVED APRIL 2, 2002
MANUSCRIPT ACCEPTED NOVEMBER 15, 2002
MANUSCRIPT HANDLED BY DARBY DYAR